Journal of Soil Sciences and Agricultural Engineering

Journal homepage: www.jssae.mans.edu.eg
Available online at: www.jssae.journals.ekb.eg

Comparison of the Effect of Air and Permeate Gap Regions on Highly Saline Water Desalination Using Hollow Fiber Membrane Distillation Modules

Abu-Zeid, M. A.*

Department of Agricultural Engineering, Faculty of Agriculture, Suez Canal University, Ismailia 41522, Egypt

ABSTRACT

The present research work discussed the impact of permeate gap region (PGR) on the high mass transfer resistance and low productivity resulted from the air gap region (AGR) sandwiched between the membrane and condensing surface in the air gap membrane distillation (AGMD). Two hollow fiber permeate gap (PGMD) and air gap membrane distillation (AGMD) modules were built, examined, and compared experimentally under several operating parameters such as feed salt concentration (C_f), feed temperature (T_f), coolant temperature (T_c), and flow rate (M_f). The performance comparison was done according to the values of energy consumption (STEC), water productivity (P_w), waste heat ($Q_{H.I}$), and gained output ratio (GOR). Results showed that the PGR was more effective than AGR on the membrane module performance at all investigated operating parameters. Under operating parameters of C_f = 7.5 g/L, T_c = 15 ºC, T_f = 70 ºC, M_f = 4 L/h, and compared with AGR, the PGR minimized STEC and $Q_{H.I}$ by around 78.32% and 47.06%, and improved the P_w and GOR by about 95.93% and 90.33%, respectively. Thus, the negative gap region effect could vanish completely by filling it with the permeated water instead of air, promoting by which the performance of the membrane distillation module remarkably.

Keywords: Air gap membrane distillation, desalination, operating parameters, permeate gap membrane distillation, performance indicators.

INTRODUCTION

One of the master prevalent problems encounters humankind all over the world is the pure water shortage and its poor quality (Voulvoulis, 2018; Anand *et al.* 2018). Membrane distillation (MD) is an effective technique used for providing pure water via saline water desalination. MD is considered a novel thermally driven process that could produce drinkable pure water with moderate operating pressure and temperature (Laganà *et al.* 2000; El-Bourawi *et al.* 2006; Alkhudhiri *et al.* 2012). The sources of low-temperature such as waste heat and solar energy could be utilized efficiently by MD technology to warm the inlet feed saline solution. Compared with other MD technologies such as sweeping gas (SGMD) (Ajdar *et al.* 2020), vacuum (VMD) (Shahu & Thombre, 2019), and direct contact membrane distillation (DCMD) (Damtie et al. 2019), the air gap membrane distillation (AGMD) is deemed the best one in terms of having low heat loss and high thermal efficiency (Gao *et al.* 2019; Abu-Zeid & ElMasry, 2020; Shahu & Thombre, 2020, 2021). However, the air gap region sandwiched between the membrane and cooling (condensing) plate decreased notably the productivity of pure drinkable water. In this context, several researchers (e.g. Ugrozov *et al.* 2003; Winter *et al.* 2011, 2012; Cipollina *et al.* 2012; Francis *et al.* 2013; Essalhi & Khayet, 2014; Khalifa 2015; Alawad & Khalifa 2019; Khalifa 2020) indicated a modern promising way to improve the productivity significantly above that of AGMD. This way represented in filling the gap region with permeated water (i.e., condensed vapor) instead of air. This new technology is named a permeate gap membrane distillation (PGMD), which is also recognized in the literature as a liquid gap (LGMD) or a water gap membrane distillation (WGMD). As presented in Figure 1 that for PGMD technology, the hot fluid communicates straightway the membrane, and due to the process of water evaporation occurring at the hot feed membrane surface, the permeated water filled the gap region and formed so-called a permeate gap region (PGR), while the cold fluid (usually the same hot saline fluid) is located on the other side of the cooling slab.

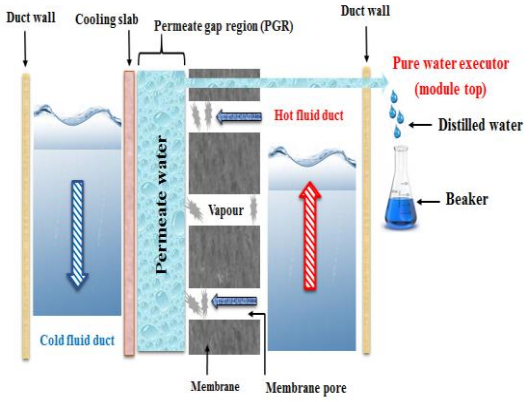

Fig.1. Permeate gap membrane distillation (PGMD).

The presence of a permeate gap region (PGR) in the modern PGMD technology helps in achievement the following features: larger internal heat recovery within the

* **Corresponding author.**
E-mail address: mostafa241981@agr.suez.edu.eg
DOI: 10.21608/jssae.2021.178723

MD module than SGMD and VMD (Winter *et al.*, 2011; Gao *et al.*, 2017), lower sensible heat loss than that of DCMD (Winter *et al.*, 2011), weak resistance to the vapor mass transfer compared with AGMD as well as the high possibility of using any other liquid as a coolant due to separation of the permeate and coolant (Winter *et al.*, 2011). In short, it could be concluded that modern PGMD technology is a mixture of various traditional MD technologies.

Some investigators (e.g. Cipollina *et al.*, 2012; Warsinger *et al.*, 2014, 2015) announced that the modern PGMD system produced greater water productivity than AGMD. In another numerical and experimental comparative investigation, Swaminathan *et al.*, (2016) proclaimed that the system of PGMD performed GOR better than AGMD by approximately 20%. Similarly, by utilizing red seawater as the feed, Francis *et al.*, (2013) revealed through a comparative study between PGMD and AGMD configurations, the new suggested PGMD configuration boosted significantly the productivity of potable water by around 820% under optimal operating conditions of gap thickness of 13 mm, the cooling temperature of 20 ºC, and feed temperature of 80 ºC. In another study, Khalifa (2015) compared experimentally the performances of the conventional AGMD and modern PGMD. The author mentioned under similar operating conditions that the new permeate gap region (PGR) formed inside the PGMD module played an important role in enhancing the heat transfer process and reducing the mass vapor transfer resistance, which promotes greatly the module productivity ranging from 90% to 140% compared to AGMD. However, the majority of PGMD researchers (e.g. Khalifa 2015; Swaminathan *et al.*, 2016; Gao *et al.*, 2017; Mahmoudi *et al.*, 2017; Cheng *et al.*, 2018; Gao *et al.*, 2019) focused on their studies in using either spiral wound or flat sheet other than the hollow fiber membrane type although a better balance could be fulfilled between the energy consumption and water productivity as mentioned by Gao *et al.*, (2017).

Therefore, due to the large specific area provided by this kind of membrane (i.e., hollow fiber) Yang *et al.*, (2011), the current research work prepared a new PGMD module fabricated by using polyvinylidene difluoride (PVDF) hollow fiber membrane.

This research work aims to discuss the effect of permeate gap region (PGR) on the high mass transfer resistance and low productivity caused by the air gap region (AGR) located between the membrane and condensing slab in the air gap membrane distillation (AGMD). So, two hollow fiber permeate gap membrane distillation (PGMD) and air gap membrane distillation (AGMD) modules were built, tested, and compared experimentally under several operating parameters including coolant temperature (T_c), feed salt concentration (C_f), flow rate (M_f), and feed temperature (T_f). This comparison was proceeded based on the obtained values of some performance indicators such as gained output ratio (GOR), energy consumption (STEC), water productivity (P_w), and waste heat ($Q_{H.I}$).

MATERIALS AND METHODS

Experimental comparison of the performance of traditional AGMD and modern PGMD for saline saline water desalination was proceeded in the period from April 2019 to January 2020 during my working as a researcher through a postdoctoral scholarship has been granted by Talent Young Scientist Program (TYSP), Beijing, China at the laboratory of Institute of Biological and Chemical Engineering, State Key Laboratory of Separation Membranes and Membrane Processes, School of Material Science and Engineering, Tiangong University, Tianjin, China.

Experimental equipment set-up and membrane materials

The flow diagrams of the designed AGMD and PGMD modules are illustrated schematically in Figure 2 (a) and (b). The two designed hollow fiber AGMD and PGMD modules having a thermostatic heating bath (Tongzhou Branch of Shanghai Jinping Instrument Limited Company, China), electronic balance, feeding tank, beaker, pump (MP-55RZ, Shanghai Xinxishan Industrial Limited Company), electric heater, valve, rotameter (LZB-4, Huanming, Yugao Industrial Automation Instrument Company, Zhejiang, China), and coolant (DLSB-10, Tianjin Xingke Instrument Limited Company, China). The two different studied AGMD and PGMD modules are similar in all components except a distilled pure water executor, where located at the module bottom in the AGMD and the module top in the PGMD as shown in Figure 2 (a) and (b).

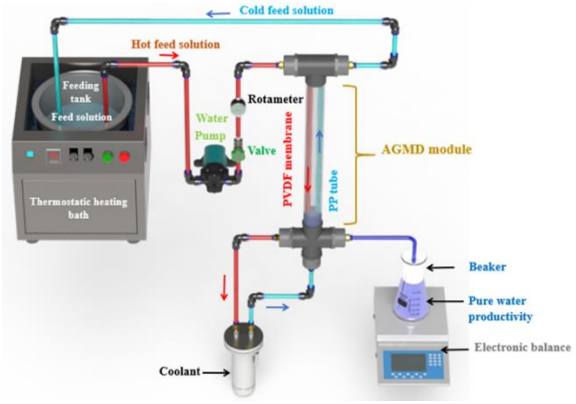

(a) AGMD

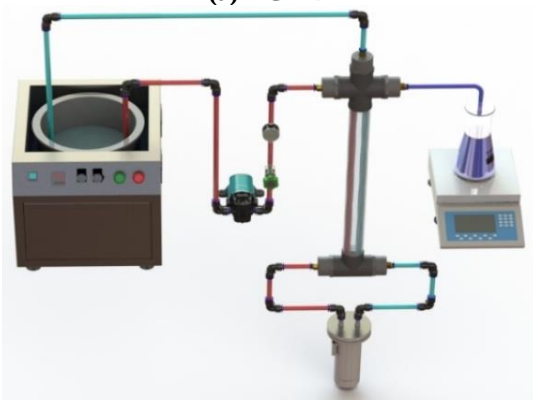

(b) PGMD

Fig.2. The flow diagrams of the (a) AGMD and (b) PGMD modules used in the experiment.

A plexiglass material was used in the preparation of the two AGMD and PGMD modules and a thermal insulation material (i.e., cotton) were utilized to decrease the heat losses from the feed circulatory to the environment. Inside each MD module, non-porous heat exchange tubes are made of polypropylene (PP) material

and micro-porous hollow fiber membranes are made of polyvinylidene difluoride (PVDF) material. The tube and membrane are arranged in a counter-current flow. The average gap thickness between the tube and membrane is ≈ 5 mm. The MD module dimensions are listed in table 1. The characteristics and specifications for each PVDF hollow fiber membrane, pump, heating bath, and coolant are tabulated in table 2.

Table 1. Dimensions of the PP tubes (non-porous) and PVDF membrane (micro-porous).

Hollow fiber types	ID / OD (mm)	Number of hollow fibers	Hollow fiber length (m)	Module length (mm)	*Inner surface area (m^2)
PP	0.40 / 0.50	240	0.59	0.77	0.18
PVDF	0.80 / 1.10	120	0.59	0.77	0.18

***The inner surface area was estimated according to the inner diameter of the PVDF and PP.**

Table 2. The specifications and characteristics of the coolant, PVDF membrane, heating bath, and pump.

Item	Value
Coolant	
Max. head (m)	3
Frequency (Hz)	50
Refrigerating capacity (KW)	0.550-0.275
Voltage (V)	220
Max. flow (L/min)	15
Power (KW)	0.23
Highest lift (m)	10
PVDF membrane	
Thickness (μm)	150
Bubble point pressure (MPa)	0.11
Porosity (%)	85
pore size (μm)	0.20
Contact angle (°)	80.5
Heating bath	
Highest temperature (°C)	95
Frequency (Hz)	50
Power (KW)	1.5
Voltage (V)	220
Pump	
Voltage (V)	220
Max. flow (L/min)	25
Highest lift (m)	10
Max. head (m)	8
Speed(rpm)	2800
Frequency (Hz)	50
Current (A)	0.95
Power (KW)	0.09

As seen in Figure 3 (a) and (b), the temperatures of hot and cold feed solution were recorded experimentally by distributing four sensors at the inlets and outlets of PVDF membrane and PP tube.

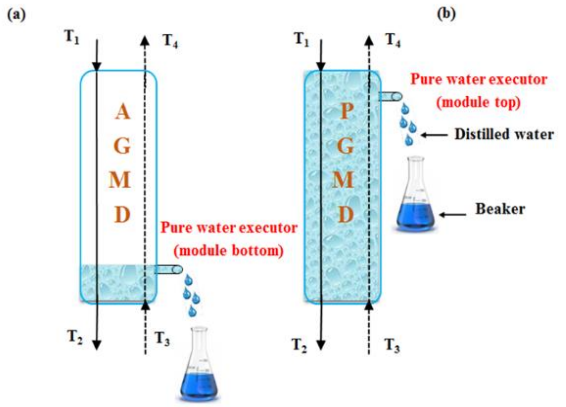

Fig.3. The difference between (a) AGMD and (b) PGMD modules with regards to the place of pure water executor.

Temperature controller XMTD-3001 (Easey Commercial Building Hennessy Road Wanchai Hongkong, China) was used to keep the temperature of inlet hot feed (T_f) constant at 40 °C, 55 °C, 70 °C, and 85 °C. The electronic balance was utilized to measure the module productivity in Kg/(m^2.h). Conductivity meter DDS-11A (Shanghai Leici Xinjing Instrument Company, China) was used to measure the electrical conductivity of pure distilled water and feed salt concentration (C_f) at 5 g/L, 10 g/L, 15 g/L, and 20 g/L. The coolant was fixed at the membrane module cold feed side to maintain the coolant temperature (T_c) stable at 5 °C, 10 °C, 15 °C, and 20 °C. Rotameter was placed in the feed line to adjust the mass flow rates of the hot feed solution (M_f) stable at 4 L/h, 8 L/h, 12 L/h, and 16 L/h.

Experimental description

Figure 2 (a) and (b) showed the steps that saline feed solution passes beginning from the feeding tank until stored ultimately in the beaker as a pure distilled water. As illustrated above in the schematic diagrams, the hot saline feed solution was transferred from the feeding tank to the membrane module by using a water pump. Then, the hot solution moved from a higher to a lower point of the PVDF membrane module where water vapor diffuses through the dry pores of the PVDF membrane. After the hot solution leaving the lower point of the membrane module entered the coolant device for a temperature reduction at the cold feed side. Then, the cold solution moved from a lower to a higher point of the PP heat exchange tubes. After the cold solution going away the higher point of the PP tubes is returned to the feeding tank for a new desalination cycle. To keep constant both volume and salt concentration of feed solution throughout the experiment, a distilled water stored in the beaker was poured into a feeding tank once again. Each experiment was repeated three times under the same inlet operating parameters for 1 h and average values were reported. Also, before initiating the experiment, the whole system of membrane distillation desalination was left working for 1 h to remove all dissolved gases in the feed solution and to reach a steady-state condition.

The MD module performance parameters

The MD module performances are evaluated via calculating energy consumption (STEC), gained output ratio (GOR), productivity (P_w), and waste heat ($Q_{H.I}$). The various values of the saline water specific heat (C_{pw}) and density (ρ) are gotten at 25 °C ambient air temperature and listed below in table 3. The various measurements involving inlet (T_1) and outlet (T_2) hot feed temperature, inlet (T_3) and outlet (T_4) cold feed temperature, and the module productivity (P_w) are written down every 10 min for 1 h and tabulated in tables 4, 5, 6, and 7 at various feed temperatures (T_f), coolant temperatures (T_c), flow rates (M_f), and salt concentrations (C_f), respectively.

Table 3. The values of density (ρ) and specific heat (C_{Pw}) at various feed concentrations (C_f).

C_f (g/L)	C_{pw} (KJ/kg.ºC)	ρ (kg/m³)
5	4.159075	1000.675
10	4.131650	1004.400
15	4.105000	1008.225
20	4.078350	1012.050

Table 4. The measured T_1, T_2, T_3, and T_4 at various feed temperatures (T_f).

T_f (ºC)	T_1	T_2	T_3	T_4
AGMD	Constant M_f = 12 L/h, C_f = 5 g/L, T_c = 15 ºC			
40	40.10	28.80	14.80	19.80
55	52.30	37.80	14.50	21.70
70	67.10	47.70	14.30	24.80
85	80.80	58.90	13.60	30.00
PGMD				
40	42.40	30.40	14.80	21.00
55	55.50	40.90	14.70	23.90
70	69.00	50.10	14.40	26.00
85	82.60	61.70	13.70	31.10

Table 5. The measured T_1, T_2, T_3, and T_4 at various coolant temperatures (T_c).

T_c (ºC)	T_1	T_2	T_3	T_4
AGMD	Constant M_f = 16 L/h, C_f = 5 g/L, T_f = 85 ºC			
5	81.90	61.20	4.50	7.70
10	82.70	62.7	9.60	15.40
15	82.50	62.30	14.60	23.00
20	80.30	60.1	19.60	26.10
PGMD				
5	84.10	63.20	4.80	10.80
10	85.30	64.70	9.80	18.70
15	84.80	64.20	14.90	25.00
20	83.90	62.70	19.80	29.60

Table 6. The measured T_1, T_2, T_3, and T_4 at various flow rates (M_f).

M_f (L/h)	T_1	T_2	T_3	T_4
AGMD	Constant T_c = 15 ºC, T_f = 70 ºC, C_f = 7.5 g/L			
4	68.50	40.00	14.50	30.20
8	68.00	42.20	14.60	28.90
12	67.60	44.20	14.60	25.10
16	66.90	46.60	14.80	23.50
PGMD				
4	71.70	43.30	14.40	32.30
8	70.20	45.20	14.50	31.20
12	69.40	47.00	14.30	28.80
16	68.00	48.30	14.90	26.70

Table 7. The measured T_1, T_2, T_3, and T_4 at various feed salt concentrations (C_f).

C_f (g/L)	T_1	T_2	T_3	T_4
AGMD	Constant T_c = 15 ºC, T_f = 55 ºC, M_f = 8 L/h			
5	52.80	36.50	14.30	25.70
10	53.30	33.30	14.60	25.90
15	52.20	35.40	14.50	25.20
20	53.60	34.20	14.00	23.80
PGMD				
5	53.60	38.90	14.50	27.00
10	55.40	37.00	14.40	27.60
15	54.80	38.20	14.30	27.30
20	55.00	36.00	13.90	26.40

The different equations used in the calculation

1. Energy consumption (MWh/Kg) (Duong *et al.* 2016):

$$STEC = \frac{M_f \times \rho \times C_{pw} \times \Delta T_{cross}}{3.6\times10^6 \times 10^3 \times P_w}$$

$$STEC = \frac{M_f \times \rho \times C_{pw} \times (T_1 - T_4)}{3.6\times10^9 \times P_w} \quad [1]$$

where ***STEC*** **is the specific thermal energy consumption,** M_f **is the mass feed flow rate (L/h),** ρ **is the density of feed saline water (kg/m³),** C_{Pw} **is the specific heat of saline water (J/kg.ºC),** ΔT_{cross} **is the temperature difference through the membrane (ºC).**

2. Pure water productivity (Kg/(m².h)):

$$P_w = \frac{W_w}{A_{iner} \times t} \quad [2]$$

where W_w **is the weight of pure water productivity within a time of** t **(Kg) and** A_{iner} **is the effective hollow fiber membrane surface area according to the inner diameter (m²).**

3. Waste heat (MJ/Kg):

$$Q_{H.I} = M_f \times C_{pw} \times \Delta T_{cross}$$

$$Q_{H.I} = M_f \times C_{pw} \times (T_1 - T_4) \quad [3]$$

4. Gained output ratio (Çengel 2003; Yao *et al.* 2012):

$$GOR = \frac{Q_{L.H.}}{Q_{H.I}} \quad [4]$$

$$Q_{L.H.} = P_w \times \Delta H_v \quad [5]$$

where Q_{LH} **is the evaporation latent heat transfer (MJ/h) and** ΔH_V **is the latent heat of vaporization (≈ 2326 kJ/kg).**

The salt rejection rate (*SRR*) in (%) could determine as:

$$SRR = \left(1 - \frac{S_w}{S_f}\right) \times 100 \quad [6]$$

where S_f **and** S_w **are the concentration of saline feed and pure water (g/L), respectively.**

RESULTS AND DISCUSSION

Comparison of the effect of AGR and PGR on the MD module performance at various feed temperatures (T_f)

Figure 4(a) elucidates the comparison of the effect of AGR and PGR on the AGMD and PGMD module's performance in terms of productivity (P_w). Experiment was proceeded as a function of feed temperature (T_f) at constant M_f = 12 L/h, C_f = 5 g/L, and T_c = 15 ºC. Experimental results present, by increasing the feed temperature (T_f) in a range of 40 ºC- 85 ºC with 15 ºC interval, the productivity (P_w) generally rise for both AGMD and PGMD modules. However, the augmentation in the productivity for the PGMD module was higher than that of the AGMD. For example, in comparison with the AGMD module, increments reached up to 62.67%, 40.97%, 23.48%, and 18.05% in the PGMD productivity were accomplished at feed temperatures (T_f) of 40 ºC, 55 ºC, 70 ºC, and 85 ºC, respectively. Abu-Zeid et al. (2020a) explained the variation in the productivity volume between PGMD and AGMD as follows: the low AGMD productivity was due to AGR which imposes a negative resistance to the vapor transfer and decreases the temperature of feed solution. While the high PGMD productivity was related mainly to the marginal impact of temperature polarization (TP) phenomena and the increase the difference in vapor pressure through the membrane fulfilled by the PGR.

It is obvious from figure 4(b), the gained output ratio (GOR) of the PGMD was found to be boosted by 54.18%, 36.49%, 21.64%, and 16.40% compared with AGMD. The main cause behind GOR augmentation was due to an effective heat recovery achieved via cold solution within the PGR raised by which the difference in temperature across the membrane ($\Delta T_{cross}=T_1-T_4$) as follows: 5.42%, 3.27%, 1.65%, and 1.38%, from AGMD to PGMD (see Table 4).

Compared with the AGR influence, the PGR diminished largely the PGMD module energy consumption (STEC) as follows: 60.00%, 47.56%, 32.43%, and 26.67% (figure 4(c)). Similarly, the waste heat ($Q_{H.I}$) was declined by 35.82%, 26.87%, 16.98%, and 13.46% (figure 4(d)).

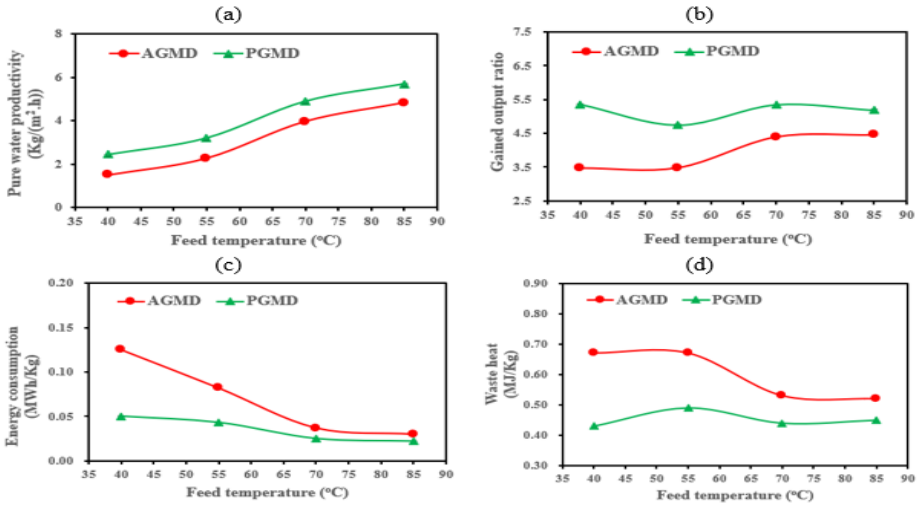

Fig.4. Effect of feed temperature on the (a) productivity (b) gained output ratio (c) energy consumption (d) and waste heat in both of AGMD and PGMD modules.

Comparison of the effect of AGR and PGR on the MD module performance at various coolant temperatures (T_c)

Figure 5(a) shows the comparison results between the AGR and PGR influence on the AGMD and PGMD performance regarding the module productivity. The experiment was done as a function of coolant temperature (T_c) at a stable M_f = 16 L/h, C_f = 5 g/L, and T_f = 85 °C. In the tested range of coolant temperature, both AGMD and PGMD modules productivity generally dropped remarkably when the coolant temperature (T_c) boosted gradually from 5 °C to 20 °C with 5 °C interval. However, the existence of PGR makes the PGMD module performance less susceptible to the coolant temperature compared with the AGMD module. As elucidated in figure 5(a), in comparison with AGMD, increases around 21.97%, 24.78%, 18.05%, and 48.15% were obtained in the PGMD productivity at T_c of 5 °C, 10 °C, 15 °C, and 20 °C, respectively. The low AGMD and high PGMD productivity attributed to the decline of the difference in the vapor pressure through the membrane. The reduction percentage in the ΔT_{cross} in the case of the AGMD module reached 26.95% corresponding to only 25.92% in the case of PGMD when the T_c increased from 5 °C to 20 °C (see Table 5). Besides, a marginal temperature polarization (TP) effect thanks to the PGR, unlike the AGR.

As for gained output ratio (GOR), results announced, by increasing the coolant temperature (T_c) in a range of 5 °C - 20 °C, the GOR mostly decreases for both AGMD and PGMD modules. However, the GOR reduction in the case of the PGMD module was lesser than that of AGMD. It is evident from figure 5(b) that the GOR was augmented by 23.40%, 26.14%,17.54%, and 48.00%, from AGMD to PGMD. The main reason behind positive GOR results was due to better heat recovery accomplished via cold feed solution within PGR. The functional internal heat recovery process was more clear in raising the temperature of T_4 and T_1 through a good blend in the feeding tank (see Table 5). Abu-Zeid *et al.* (2020b) translated the negative GOR results for AGMD for two possible reasons. Firstly, poor cooling for vapor molecules because of specific heat capacity of air (i.e., $C_{p\,air}$ = 993 J/kg.°C) lesser than water ($C_{p\,water}$ = 4200 J/kg.°C). Secondly, lowering the ratio of heat used to produce distilled water and heat used for warming the feed solution.

The PGR decreased significantly the PGMD module energy consumption (STEC) by 35.29%, 37.04%, 27.66%, and 54.01% compared with AGMD (figure 5(c)). Also, PGR declined the module waste heat ($Q_{H.I}$) as follows: 18.18%, 21.21%, 15.85%, and 32.33% (figure 5(d)). Abu-Zeid *et al.* (2020b) attributed the desired STEC and $Q_{H.I}$ value the vital role of PGR in enhancing the internal heat recovery process within the membrane module as well as the positive GOR values.

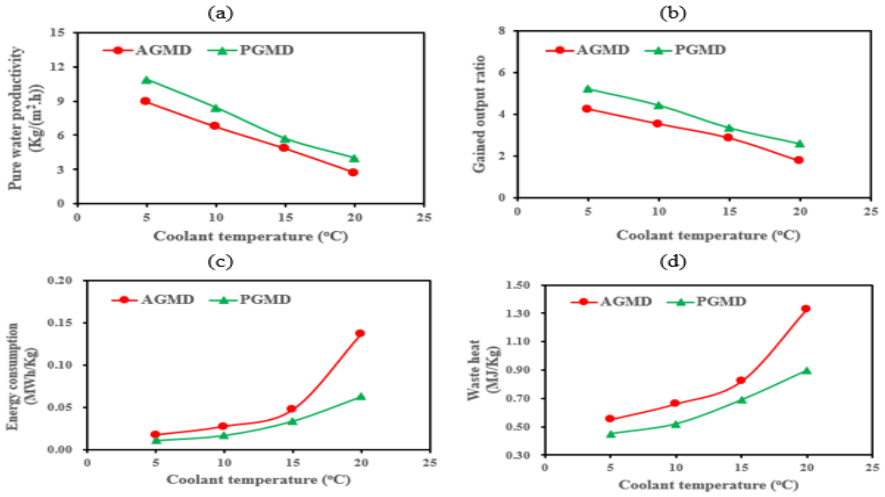

Fig.5. Effect of coolant temperature on the (a) productivity (b) gained output ratio (c) energy consumption (d) and waste heat in both of AGMD and PGMD modules.

Comparison of the effect of AGR and PGR on the MD module performance at various feed flow rates (M_f)

Figure 6(a–d) displayed the change of the energy consumption, water productivity, gained output ratio, and waste heat that happened within AGMD and PGMD modules. Experiments were performed at mass flow rates (M_f) of 4 L/h, 8 L/h, 12 L/h, and 16 L/h, and stable T_c = 15 ºC, C_f = 7.5 g/L, and T_f = 70 ºC. In comparison with AGMD, figure 6(a) declared that the PGR enhanced significantly the PGMD productivity by about 95.93%, 67.24%, 23.48%, and 34.52% at M_f of 4 L/h, 8 L/h, 12 L/h, and 16 L/h, respectively. Two reasons behind the productivity enhancement. Firstly, the weak resistance to the evaporated molecules which condenses immediately at the membrane/permeate gap interface. Secondly, reduce the thickness of the thermal boundary layer at the hot membrane surface (Abu-Zeid *et al.* 2020b, c).

Concerning GOR, augmentations of 90.33%, 67.86%, 23.41%, and 34.48% were fulfilled from AGMD to PGMD as presented in figure 6(b). Several reasons could be mentioned for GOR improvement: low conductive heat loss across the membrane, high amount of heat absorbed by the cold solution, reduce the thickness of the thermal boundary layer, and insignificant change in the mass and heat transfer process due to PGR (Abu-Zeid *et al.* 2020c).

The high GOR values reflected positively on the amount of energy consumption and waste heat. As can be shown in figures 6(c) and 6(d), the PGR decreased the STEC of the PGMD module by 78.32%, 64.18%, 37.84%, and 46.88%, and QH.I by 47.06%, 40.00%, 22.64%, and 28.30%.

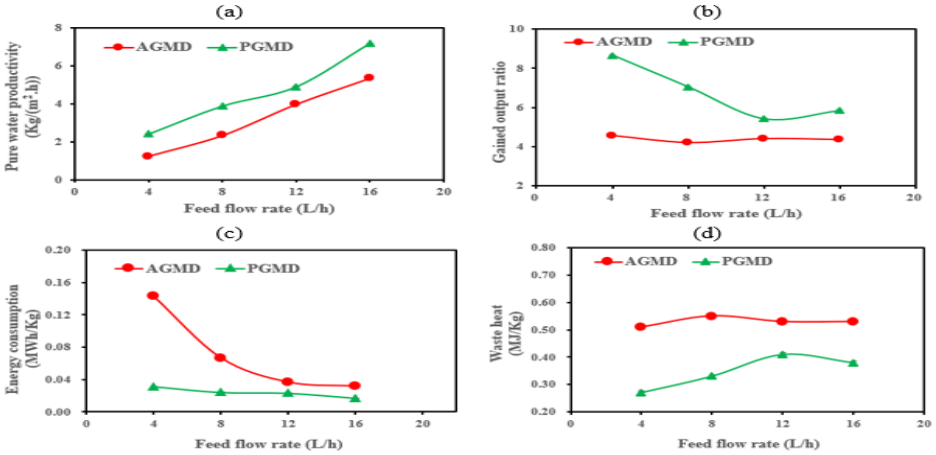

Fig.6. Effect of feed flow rate (M_f) on the (a) productivity (b) gained output ratio (c) energy consumption (d) and waste heat in both of AGMD and PGMD modules.

Comparison of the effect of AGR and PGR on the MD module performance at various feed salt concentrations (C_f)

Figure 7(a–d) illustrated the influences of PGR and AGR on the PGMD and AGMD performance at different feed salt concentrations. Experiment was done at T_c = 15 ºC, M_f = 8 L/h, and T_f = 55 ºC. As revealed in figure 7(a), augmentations around 17.34%, 40.97%, 35.80%, and 37.11% were accomplished in PGMD productivity compared with AGMD at C_f of 5 g/L, 10 g/L, 15 g/L, and 20 g/L, respectively. The improved productivity associated with a high-pressure difference through the membrane and modest concentration polarization (CP) phenomena influence at the hot feed side by dint of PGR (Abu-Zeid *et al.* 2020a, c).

Increases of 19.59%, 38.94%,33.41%, and 43.10% in the GOR values were achieved from AGMD to PGMD (figure 7(b)). Concerning the module energy consumption (STEC), the PGR minimized the STEC of the PGMD module by 31.25%, 48.98%, 45.26%, and 49.14% compared with AGMD as seen in figure 7(c). Also, the waste heat (QH.I) of the PGMD module was reduced around 17.39%, 27.50%, 25.45%, and 30.00% (figure 7(d)).

Regarding the salt rejection rate (SRR), the two AGMD and PGMD modules with hollow fiber PVDF membrane introduced high SRR ranged between 99.30% and 100% when the salt concentration of feed (C_f) raised gradually from 5 g/L to 20 g/L.

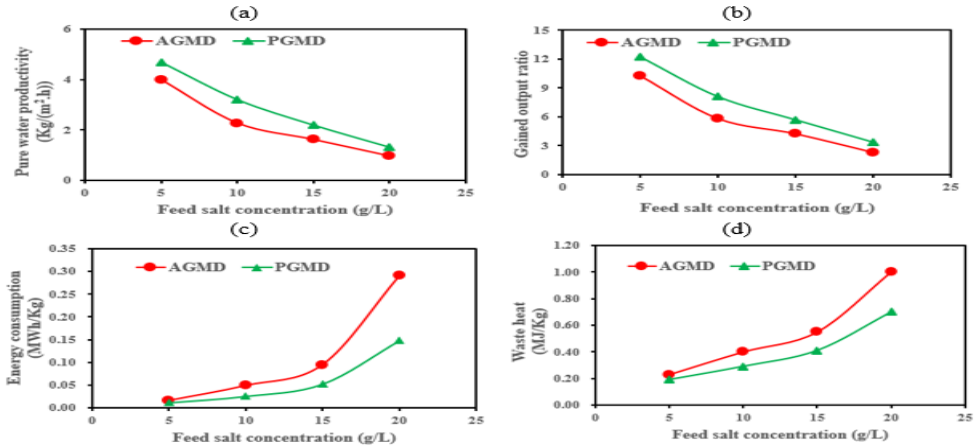

Fig.7. Effect of feed salt concentration (C_f) on the (a) productivity (b) gained output ratio (c) energy consumption (d) and waste heat in both of AGMD and PGMD modules.

CONCLUSION

The current research work discussed practically mitigating the troubles of high mass vapor transfer resistance and low productivity caused by the air gap region (AGR) sandwiched between the membrane and condensing plate via creating a new permeate gap region (PGR). The performance of a new permeate gap membrane distillation (PGMD) module having PGR was evaluated by comparing it with the conventional air gap membrane distillation (AGMD) having AGR with regards to energy consumption (STEC), water productivity (P_w), heat input ($Q_{H.I}$), and gained output ratio (GOR). It was found from the experimental results that the modern PGMD technology achieved significant increases up to 62.67%, 40.97%, 23.48%, and 18.05% in the module productivity at different feed temperatures (T_f) of 40 ^oC, 55 ^oC, 70 ^oC, and 85 ^oC, respectively compared with AGMD module at various operating parameters of coolant temperature (T_c) of 15 ^oC, feed flow rate (M_f) of 12 L/h, and salt concentration (C_f) of 5 g/L. Also, the PGR enhanced the PGMD gained output ratio (GOR) by about 54.18%, 36.49%, 21.64%, and 16.40%. Correspondingly, it reduced meaningfully the total module energy consumption (STEC) and waste heat ($Q_{H.I}$) as follows: 60.00%, 47.56%, 32.43%, and 26.67% (STEC), 35.82%, 26.87%, 16.98%, and 13.46% ($Q_{H.I}$), respectively.

ACKNOWLEDGMENT

The author would like to gratefully acknowledge the National Basic Research Program of China (No. 2015CB655303), the National Natural Science Foundation of China (No. 21076176), the National Key Technologies R&D Program (2015ZX07406006).

REFERENCES

Abu-Zeid, M. A. E. -R. & ElMasry, G. 2020. Experimental evaluation of two consecutive air-gap membrane distillation modules with heat recovery. *Water Science & Technology: Water Supply*, 20 (5): - ١٦٧٨– ١٦٩١.

Abu-Zeid, M. .A .E-R., Lu, X. &Zhang , S. 2020a. Enhancement of the air gap membrane distillation system performance by using the water gap module. *Water Science & Technology: Water Supply*, 20 (7), 2884 – 2902.

Abu-Zeid, M. .A .E-R., Lu, X. &Zhang , S. 2020b. Developing symmetrical traditional double-stage membrane distillation system based on air-gap and water-gap configurations. *Desalination and. Water Treat*ment, 202, 121 – 132.

Abu-Zeid, M. .A .E-R., Lu, X. &Zhang , S. 2020c.A novel internal heat recycling concept for reducing energy consumption and increasing flux through three-stages air-gap-water-gap membrane distillation system. *Water Science & Technology: Water Supply*, 20 (7), 2858 – 2874.

Alkhudhiri, A., Darwish, N. & Hilal, N. 2012. Membrane distillation: a comprehensive review. *Desalination*, 287, 2– 18.

Ajdar, M., Azdarpour, A., Mansourizadeh, A. & Honarvar, B. 2020. Improvement of porous polyvinylidene fluoride-co-hexafluropropylene hollow fiber membranes for sweeping gas membrane distillation of ethylene glycol solution. *Chinese Journal of Chemical Engineering*, 28 (12), 3002–3010.

Alawad, S. M. & Khalifa, A. E. 2019. Analysis of water gap membrane distillation process for water desalination. *Desalination*, 470, 114088.

Anand, A., Unnikrishnan, B., Mao, J. Y., Lin, H. J. & Huang, C. C. 2018. Graphene-based nanofiltration membranes for improving salt rejection, water flux and antifouling - A review. *Desalination*, 429, 119–133.

Çengel, Y. A. 2003. Heat Transfer: A Practical Approach. McGraw-Hill.

Cipollina, A., Di Sparti, M. G., Tamburini, A. & Micale, G. 2012. Development of a membrane distillation module for solar energy seawater desalination. Chem. *Eng. Res. Des.*, 90, 2101–2121.

Cheng, L., Zhao, Y., Li, P., Li, W. & Wang, F. 2018. Comparative study of air gap and permeate gap membrane distillation using internal heat recovery hollow fiber membrane module. *Desalination*, 426, 42–49.

Damtie, M. M., Woo, Y. C., Kim, B., Park, K.-D., Hailemariam, R. H., Shon, H. K. & Choi, J.-S. 2019. Analysis of mass transfer behavior in membrane distillation: Mathematical modeling under various conditions. *Chemosphere*, 236, 124289.

Duong, H. C., Cooper, P., Nelemans, B., Cath, T. Y. & Nghiem, L. D. 2016. Evaluating energy consumption of air gap membrane distillation for seawater desalination at pilot scale level. *Separation and Purification Technology*, 166, 55–62.

Essalhi, M. & Khayet, M. 2014. Application of a porous composite hydrophobic/hydrophilic membrane in desalination by air gap and liquid gap membrane distillation: a comparative study. *Separation and Purification Technology*, 133, 176–186.

El-Bourawi, M., Ding, Z., Ma, R. & Khayet, M. 2006. A framework for better understanding membrane distillation separation process. *Journal of Membrane Science*, 285, 4-29.

Francis, L., Ghaffour, N., Alsaadi, A. A. & Amy, G. L. 2013. Material gap membrane distillation: A new design for water vapor flux enhancement. *Journal of Membrane Science*, 448, 240–247.

Gao, L., Zhang, J., Gray, S. & Li, J.-D. 2017. Experimental study of hollow fiber permeate gap membrane distillation and its performance comparison with DCMD and SGMD. *Separation and Purification Technology*, 188, 11–23.

Gao, L., Zhang, J., Gray, S. & Li, J.-D. 2019. Influence of PGMD module design on the water productivity and energy efficiency in desalination. *Desalination*, 452, 29–39.

Khalifa, A. E. 2020. Flux enhanced water gap membrane distillation process-circulation of gap water. *Separation and Purification Technology*, 231, 115938.

Khalifa, A. E. 2015. Water and air gap membrane distillation for water desalination – an experimental comparative study. *Separation and Purification Technology*, 141, 276–284.

Laganà, F., Barbieri, G. & Drioli, E. 2000. Direct contact membrane distillation: modelling and concentration experiments. *Journal of Membrane Science*, 166, 1–11.

Mahmoudi, F., Siddiqui, H., Pishbin, M., Goodarzi, G., Dehghani, S., Date, A. & Akbarzadeh, A. 2017. Sustainable seawater desalination by permeate gap membrane distillation technology. *Energy Procedia*, 110, 346–351.

Shahu, V. T. & Thombre, S. B. 2021. Experimental analysis of a novel helical air gap membrane distillation system. *Water Science & Technology: Water Supply*, 361–371.

Shahu, V. T. & Thombre, S. B. 2020. Analysis and optimization of a new cylindrical air gap membrane distillation system. *Water Science & Technology: Water Supply*, 20 (1), 361– 371.

Shahu, V. T. & Thombre, S. B. 2019. Air gap membrane distillation: a review. *Journal of Renewable and Sustainable Energy*, 11, 45901.

Ugrozov, V. V., Elkina, I. B., Nikulin, V. N. & Kataeva, L. I. 2003. Theoretical and experimental research of liquid-gap membrane distillation process in membrane module. *Desalination*, 157, 325–331.

Voulvoulis, N. 2018. Water reuse from a circular economy perspective and potential risks from an unregulated approach. *Curr. Opin. Environ. Sci. Heal.*, 2, 32-45.

Warsinger, D., Swaminathan, J., Maswadeh, L. & Lienhard V, J. H. 2015. Superhydrophobic condenser surfaces for air gap membrane distillation. *Journal of Membrane Science*, 492, 578–587.

Warsinger, D. E. M., Swaminathan, J. & Lienhard V, J. H. 2014. Effect of module inclination angle on air gap membrane distillation, in: Proceedings of the 15th International Heat Transfer Conference, IHTC-15, Paper No. IHTC15-9351, Kyoto, Japan.

Winter, D., Koschikowski, J. & Ripperger, S. 2012. Desalination using membrane distillation: flux enhancement by feed water deaeration on spiral-wound modules. *Journal of Membrane Science*, 423–424, 215–224.

Winter, D., Koschikowski, J. & Wieghaus, M. 2011. Desalination using membrane distillation: experimental studies on full scale spiral wound modules. *Journal of Membrane Science*, 375, 104–112.

Swaminathan, J., Chung, H. W., Warsinger, D. M., AlMarzooqi, F. A., Arafat, H. A. & Lienhard V, J. H. 2016. Energy efficiency of permeate gap and novel conductive gap membrane distillation. *Journal of Membrane Science*, 502, 171–178.

Yang, X., Wang, R., Shi, L., Fane, A. G. & Debowski, M. 2011. Performance improvement of PVDF hollow fiber-based membrane distillation process. *Journal of Membrane Science*, 369, 437–447.

Yao, K., Qin, Y. J., Yuan, Y. J., Liu, L. Q., He, F. & Wu, Y. 2012. A continuous-effect membrane distillation process based on hollow fiber AGMD module with internal latent-heat recovery. *AlChE Journal*, 59 (4), 1278–1297.

مقارنة تأثير منطقة الفجوة الهوائية والمائية علي تحلية المياة عالية الملوحة بإستخدام وحدات التقطير الغشائي ذو الألياف المجوفة

مصطفى عبدالراضى أبوزيد

قسم الهندسة الزراعية ، كلية الزراعة ، جامعة قناة السويس ، الاسماعيلية ، مصر

يناقش العمل البحثي الحالي تأثير منطقة الفجوة المائية علي كلا من المقاومة العالية لإنتقال الكتلة والإنتاجية المنخفضة الناتجة عن تأثير منطقة الفجوة الهوائية المتواجد بين الغشاء وسطح التكثيف (التبريد) في وحدة التقطير الغشائي ذو الفجوة الهوائية. تم خلال العمل التجريبي الحالي بناء وإختبار ومقارنة وحدتي التقطير الغشائي ذو الفجوة الهوائية والمائية عند بارامترات تشغيل عديدة مثل تركيز الأملاح في الماء المغذي ودرجة حرارة الماء المغذي ودرجة حرارة التبريد ومعدل التدفق. هذا وقد تم مقارنة الأداء لهذة الوحدات وفقا للقيم المختلفة المتحصل عليها لكلا من إستهلاك الطاقة والإنتاجية والحرارة المفقودة وكفاءة الطاقة. أوضحت النتائج المتحصل عليها أن منطقة الفجوة المائية كانت أكثر تأثيرا وفعالية علي أداء وحدة التقطير الغشائي مقارنتا بمنطقة الفجوة الهوائية عند كل بارامترات التشغيل المختبرة. حيث وجد أنة عند تركيز أملاح ٧,٥ جم/لتر ودرجة حرارة تبريد ١٥ درجة مئوية ودرجة حرارة ماء مغذي ٧٠ درجة مئوية ومعدل تدفق ٤ لتر/ساعة ومقارنتا بمنطقة الفجوة الهوائية أن منطقة الفجوة المائية قد قللت كثيرا من إستهلاك الطاقة والحرارة المفقودة بنسبة وصلت إلي % ٧٨,٣٢ و % ٤٧,٠٦ وحسنت كلا من الإنتاجية وكفاءة الطاقة بنسبة وصلت إلي % ٩٥,٩٣ و % ٩٠,٣٣ علي التوالي. وعلية فإنة يمكننا القول أنة بناءا علي النتائج الإيجابية المتحصل عليها أن التأثير السلبي لمنطقة الفجوة يمكن أن يتلاشي تماما بواسطة ملئ هذة المنطقة بالماء بدلا من الهواء مما يحسن بشكل ملحوظ أداء وحدة التقطير الغشائي.